

Label-Leaks: Membership Inference Attack with Label

Zheng Li and Yang Zhang
CISPA Helmholtz Center for Information Security

Abstract—Machine learning (ML) has made tremendous progress during the past decade and ML models have been deployed in many real world applications. However, recent research has shown that ML models are vulnerable to attacks against their underlying training data. One major attack in this field is membership inference the goal of which is to determine whether a data sample is part of the training set of a target machine learning model. So far, most of the membership inference attacks against ML classifiers leverage the posteriors returned by the target model as their input. However, empirical results show that these attacks can be easily mitigated if the target model only returns the predicted label instead of posteriors.

In this paper, we perform a systematic investigation of membership inference attack when the target model only provides the predicted label. We name our attack label-only membership inference attack. We focus on two adversarial settings and propose different attacks, namely transfer-based attack and perturbation based attack. The transfer-based attack follows the intuition that if a locally established shadow model is similar enough to the target model, then the adversary can leverage the shadow model’s information to predict a target sample’s membership. The perturbation-based attack relies on adversarial perturbation techniques to modify the target sample to a different class, and uses the magnitude of the perturbation to judge whether it is a member or not. This is based on the intuition that a member sample is harder to be perturbed to a different class than a non-member sample. Extensive experiments over 6 different datasets demonstrate that both of our attacks achieve strong performance. This further demonstrates the severity of membership privacy risks of machine learning models.

I. INTRODUCTION

Over the past decade, machine learning (ML) has witnessed tremendous progress, enabling a wide range of applications, such as image recognition and machine translation. However, various recent research has shown that machine learning models are vulnerable to attacks against their training data [11], [14], [18]–[20], [24], [33], [37], [43], [44], [46], [48]. One major attack in this field is the membership inference attack which aims to determine whether a data sample is used to train a target ML model or not. Successful membership inference attacks can lead to severe consequences. For instance, if a machine learning model is trained on data collected from patients with a certain disease, then knowing a victim belonging to the training set immediately leaks the health status of the victim.

All the current membership inference attacks leverage the overfitting nature of ML models. Specifically, an ML model is more confident facing a data sample it was trained on, and this confidence is reflected on the model’s output, i.e., posteriors in the ML classification setting. Therefore, they use the posteriors of the target sample returned by the target model as their attack models’ input. We refer to these attacks as *posterior-based membership inference attacks*.

A major drawback for the current posterior-based attacks

is that they can be trivially mitigated [32], [46], [48], [57]: The model can simply return the predicted label instead of posteriors. The fact that posterior-based attacks can be easily averted makes it more difficult to evaluate whether a model is truly vulnerable to membership inference or not, which may lead to premature claims about the model’s privacy risks.

A. Our Contributions

In this paper, we study membership inference attack against machine learning models when the target model *only* provides the predicted label of the target sample instead of posteriors. We name our attack *label-only membership inference attack*.

Specifically, we study two different scenarios for label-only membership inference and propose two attacks, namely *transfer-based membership inference attack* and *perturbation-based membership inference attack*. For both of our attacks, we consider an adversary with only black-box access to the target model. This means that the adversary can only query the model with a set of data samples and obtain the corresponding predicted labels, i.e., the most difficult setting for the adversary [48]. In the following, we abstractly introduce each of our attacks.

Transfer-based Membership Inference Attack. For the transfer-based membership inference attack, we assume that the adversary has a shadow dataset that comes from the same distribution as the target model’s training set. However, the adversary does not know the ground truth labels for samples in the shadow dataset. We first use the target model as an oracle to label samples in the shadow dataset. In this way, we hope the labelled shadow dataset can contain enough information from the target model. Then, we use the shadow dataset to construct a shadow model to mimic the target model. In the end, we rely on the shadow model to perform our attack following the intuition that if the shadow model is similar enough to the target model, then a target sample being predicted confidently by the shadow model indicates it is a member of the target model’s training set.

Extensive experimental evaluation (we use a set of models with different overfitting levels under multiple types of datasets) shows that the adversary can achieve excellent membership inference performance. For instance, we achieve an AUC (area under the ROC curve) of 0.8749 when the target model is trained with the CIFAR-10 dataset [1].

Perturbation-based Membership Inference Attack. For this adversary, we consider a more difficult and realistic scenario in which no shadow dataset is available to the adversary. To compensate for the lack of information in this setting, we shift our focus from the model’s output to the input. Here, our intuition is that it is harder to perturb a member sample to a different class than a non-member sample relying on

TABLE I: An overview of the different types of membership inference attacks. “✓” means the adversary needs the information and “-” indicates the information is not necessary.

Attack category	Attacks	Target model’s structure	Target model’s training data distribution	Detailed model prediction (e.g. probabilities or logits)	Predicted label
Posterior-based	[32], [46], [48], [57]	✓ or -	✓ or -	✓	✓
Label-only	Transfer-based	-	✓	-	✓
	Perturbation-based	-	-	-	✓

adversarial example techniques. Following this intuition, the adversary use the magnitude of the perturbation to differentiate member and non-member samples.

Experimental evaluations show that the perturbation-based attack has excellent performance on multiple datasets, and in some cases is even better than the transfer-based attack. For instance, our attack achieves an AUC of 0.7988 on the MNIST dataset [2], and an AUC of 0.9216 on the CIFAR-10 dataset. We further conduct experiments to prove the feasibility of this method and reveal the reasons behind the attack’s success.

Our results show that membership inference can be effectively mounted when the target model only provides the predicted label. This further sheds light on the severe privacy risks caused by membership inference attacks against ML models.

In general, our contributions can be summarized as the following:

- We perform a systematic investigation on label-only membership inference attack against machine learning models, which is highly relevant for real-world applications and important to gauge model privacy.
- We introduce two label-only membership inference attacks under two different attack scenarios, including transfer-based attack and perturbation-based attack.
- Extensive experiments on a wide range of datasets demonstrate the severe membership privacy risks stemming from machine learning models.

B. Organization

The rest of the paper is organized as the following. Section II introduces the definition of membership inference against ML models, target models, and datasets used in the paper. Section III and Section IV present the threat models, attack methodologies, and evaluations of our two types of attacks, respectively. In Section V, we discuss the limitations of the current work and possible extensions. Section VI presents the related work and Section VII concludes the paper.

II. PRELIMINARIES

In this section, we first define the membership inference attack in the machine learning setting, second, describe the datasets used, and third, introduce the target model used for our evaluation.

A. Membership Inference Against Machine Learning Models

In this paper, we concentrate on machine learning classification, the most common ML application. An ML classifier \mathcal{M} aims to map a data sample $x \in \mathcal{X} \subset \mathbb{R}^d$ to a class label $y \in \{1, 2, \dots, K\}$. Here, K represents the total number of labels. For most of the classification models, the output vector $\mathcal{M}(x)$ can be interpreted as a set of posterior probabilities over all classes, and the sum of all the values is 1. We also refer to this vector as posteriors. To learn an ML classifier, one needs a labelled dataset and performs optimization following a predefined loss function.

Membership inference attack in the ML setting emerges when an adversary aims to find out whether her target data sample is used to train a certain ML model. More formally, given a data sample x , a trained machine learning model \mathcal{M} , and external knowledge of an adversary, denoted by Ω , a membership inference attack (*attack model*) can be defined as the following function.

$$\mathcal{A} : x, \mathcal{M}, \Omega \rightarrow \{0, 1\}$$

Here, 0 means x is not a member of \mathcal{M} ’s training dataset \mathcal{D}_{Train} and 1 otherwise. The machine learning model \mathcal{M} that the adversary targets is also referred to as the *target model*.

The attack model \mathcal{A} is essentially a binary classifier. Depending on the assumptions, it can be constructed in different ways, which will be presented in later sections.

B. Datasets Description

We utilize 6 different benchmark image datasets, including MNIST [2], FashionMNIST [3], CIFAR-10 [1], CIFAR-100 [1], GTSRB [4], and Face [5], to conduct our experiments. For each dataset, we split it by half into \mathcal{D}_{Target} and \mathcal{D}_{Shadow} : One is used to train the target model, while the other is used to train the shadow model for our transfer-based attack. As images in GTSRB are different size, we resize them to 64×64 pixels. For the Face dataset, we only consider people with more than 40 images, which leaves us with 19 peoples data, i.e., 19 classes.

C. Target Model Description

Generally, we use convolutional neural network (CNN) for image classification tasks, which is also the network architecture adopted by previous works [34], [35], [46], [48]. For MNIST and FashionMNIST, since they are only 28×28 grayscale images, our CNN is assembled with 2 convolutional layers and 2 pooling layers with 1 hidden layer containing 784 units in the end. For the other datasets, we use 10 convolutional layers and 5 pooling layers with 2 hidden layers containing 256 units each in the end.

TABLE II: Target model \mathcal{M} with different overfitting levels on each dataset. We split each dataset to training and testing set with different fractions.

Target Model	Target Dataset					
	MNIST	FMNIST	CIFAR10	CIFAR100	GTSRB	Face
\mathcal{M} -0	0.09	0.17	0.36	0.65	0.26	0.14
\mathcal{M} -1	0.12	0.18	0.40	0.68	0.39	0.20
\mathcal{M} -2	0.15	0.22	0.44	0.73	0.46	0.27
\mathcal{M} -3	0.17	0.24	0.50	0.77	0.55	0.35
\mathcal{M} -4	0.29	0.29	0.58	0.80	0.67	0.43
\mathcal{M} -5	0.38	0.41	0.63	0.83	0.76	0.55

It is well known that overfitting drives classifiers to be vulnerable to membership inference attacks [46], [48]. To show the variation of the attack performance on each dataset, we build models with different overfitting levels. In particular, we train the target model using dataset of different size (detailed in the Appendix). And, we quantify the overfitting level of a target model as the difference between its prediction accuracy on the training set and testing set. All the target models with different overfitting levels on each dataset are summarized in Table II.

III. TRANSFER-BASED MEMBERSHIP INFERENCE ATTACK

In this section, we present the first attack, i.e., transfer-based membership inference. We start by introducing the threat model. Then, we describe the attack methodology. In the end, we present the evaluation results.

A. Threat Model

As presented in Table I, the adversary only has black-box access to the target model, i.e., she is not able to extract the target sample’s membership status from the posteriors. Therefore, the adversary trains a shadow model \mathcal{S} to imitate the behavior of the target model \mathcal{M} , and then relies on the shadow model to mount the attack.

To train the shadow model, we assume that the adversary has a unlabelled shadow dataset, denoted by \mathcal{X}_{Shadow} that comes from the same underlying distribution as the target model’s training set \mathcal{D}_{Target} . This is a weaker assumption compared to previous works [46], [48] and renders the adversary more flexibility.

B. Key Intuition

Our intuition for this attack can be described as the following proposition.

Proposition 1. If the shadow model \mathcal{S} and the target model \mathcal{M} are similar enough, then a data sample’s membership status in the target model can be reflected in the shadow model.

Following this intuition, we hypothesize that if the target sample receives a confident prediction on the shadow model, then it is likely to be a member in the target model’s training set. To quantify the prediction confidence of the target sample on the shadow model \mathcal{S} , we focus on its loss with respect to \mathcal{S} . Besides, we also consider the maximal posterior and posterior entropy. Note that the target sample is never used to train the shadow model.

C. Methodology

The adversary’s methodology can be divided into four stages, including shadow dataset labeling, shadow model structure selection, shadow model training, and membership inference.

Shadow Dataset Labeling. As mentioned before, the adversary has a shadow dataset \mathcal{X}_{Shadow} without labels. To train a shadow model, the first step is to label these samples using the target model \mathcal{M} as an oracle. In this way, she establish a connection between the shadow dataset and the target model, which facilitates the shadow model to be more similar to the target model.

Shadow Model Structure Selection. Since the adversary knows the main task of the target model, she simply use a similar type of neural network as her shadow model. For instance, if the target model is a convolutional neural network (CNN), then she uses a CNN as well. We emphasize that the adversary does not have the knowledge of the concrete architecture of the target model, this is another relaxed assumption compared to previous works [46], [48]. In Section III-D, we show that a wide range of architecture choices yield similar attack performance.

Shadow Model Training. The adversary trains the shadow model \mathcal{S} with the dataset and model determined in the previous two steps.

Membership Inference. Finally, the adversary feeds the target sample into the shadow model \mathcal{S} to calculate its cross-entropy loss. If the loss value is smaller than a threshold, we predict the target sample being a member and vice versa. Here, the loss value is calculate by the ground truth label of the target sample. The adversary can pick her threshold depending on her requirements, as in many machine learning applications [46]. In our evaluation, we mainly use area under the ROC curve (AUC) which is threshold independent as our evaluation metric.

D. Evaluation

Experimental Setup. We evaluate our attack over all datasets. For each dataset, we first split it by half into \mathcal{D}_{Target} and \mathcal{X}_{Shadow} .¹ Following the attack strategy, \mathcal{D}_{Target} is also split by two: One is used to train the target model \mathcal{M} , i.e., \mathcal{D}_{Train} , and serves as the member samples of the target model, while the other \mathcal{D}_{Test} serves as the non-member samples. As mentioned in Section II, for each dataset, we repeat the split 6 times with different training set proportions and then train 6 target models with different overfitting levels, denoted by \mathcal{M} -0, \mathcal{M} -1, \dots \mathcal{M} -5 (see Table II). \mathcal{X}_{Shadow} , on the other hand, is first labelled by the target model, then is used to train the shadow model.

We execute the evaluation on randomly reshuffled data samples from \mathcal{D}_{Target} , and use sets of the same size (i.e., equal number of members and non-members) to maximize the uncertainty of inference, thus the baseline performance

¹We discard the labels for \mathcal{X}_{Shadow} .

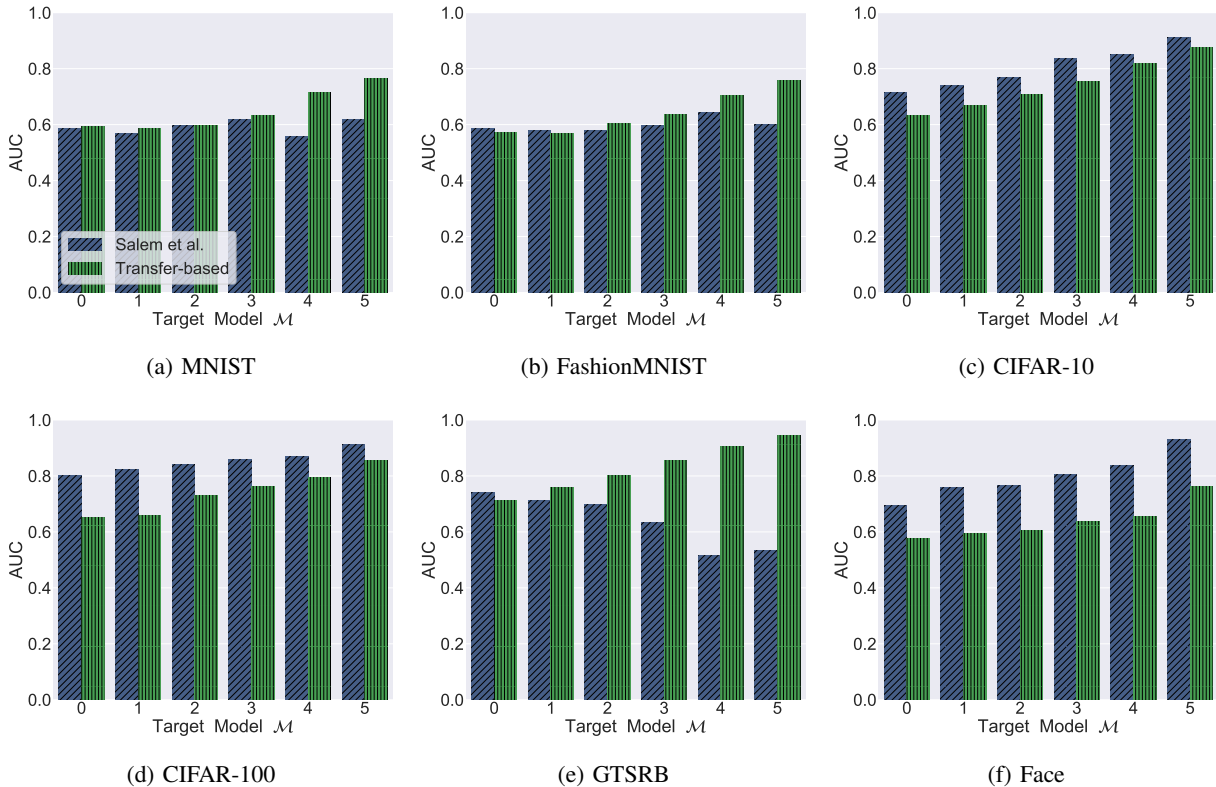


Fig. 1: Comparison of our transfer-based attack performance with the attack by Salem et al. across all target models. The x-axis represents the target model being attacked and the y-axis represents the AUC score.

is equivalent to random guessing. Note that most of the experiments by Shokri et al. [48] and Salem et al. [46] use the same setup.

We also compare our attack against the attack of Salem et al. [46]. Following the original configuration of the authors code,² we train one shadow model using half of \mathcal{X}_{Shadow} with its ground truth labels, and one attack model in a supervised manner based on the shadow model’s posteriors.

We adopt AUC as our evaluation metric which measures the area under the ROC curve. ROC reflects the relation between false positive rate and true positive rate over a set of thresholds, thus AUC is threshold independent. Many recent works have adopted AUC to measure privacy as well [8], [19], [22], [27], [41], [46]. In addition, we further discuss methods to pick threshold for our attacks in Section V.

Results. Figure 1 depicts the performance of the transfer-based attack. We observe that our attack performs relatively worse on CIFAR-10, CIFAR-100, and Face than the attack of Salem et al. [46], which is expected as their attack utilizes the posterior as the input. However, on the other 3 datasets, their attack achieves a relatively weaker performance, and even the attack performance drops with the increase of overfitting level on the GTSRB dataset (see Figure 1e). This is still due to the inherent overfitting nature of ML models, in this case the attack model. In the work by Salem et al. [46], the shadow

model is trained using the ground truth labels from the shadow dataset rather than the target model’s outputs, which indicates the training process is independent of the target model. Further, this also shows that the closer the overfitting level between the shadow model and the target model, the more similar the posterior distribution between them, then a more effective attack model can be achieved.³ However, the adversary cannot determine the precise overfitting level of the target model in real-world applications, which lead to a huge uncertainty of the attack performance, as shown in Figure 1c, Figure 1d, and Figure 1e.

We further investigate the effect of the shadow dataset size and shadow model complexity (structure and hyper-parameter) on the attack performance. More concretely, we vary the size of the shadow dataset \mathcal{X}_{Shadow} from 1,920 to 19,200, where the target training set \mathcal{D}_{Train} is 9,600. We also vary the complexity of the shadow model from 3.85M (number of parameters) and 40.15M (FLOPs, computational complexity) to 24.91M and 446.85M, where the target model complexity is 9.56M and 229.54M, respectively. We conduct an extensive experiment to tune these two hyperparameters simultaneously and report the results in Figure 3. Through investigation, we make the following observations.

- Larger shadow dataset implies more queries to the target model which leads to better attack performance.

²<https://github.com/AhmedSalem2/ML-Leaks>

³We confirm this with the authors.

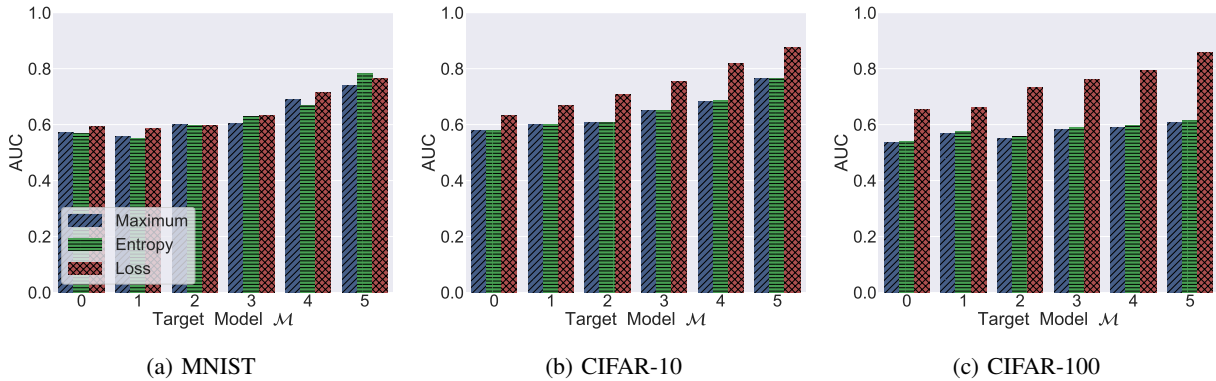


Fig. 2: Attack AUC for three different statistical measures over all datasets and target models. The x-axis represents the target model being attacked and the y-axis represents the AUC score.

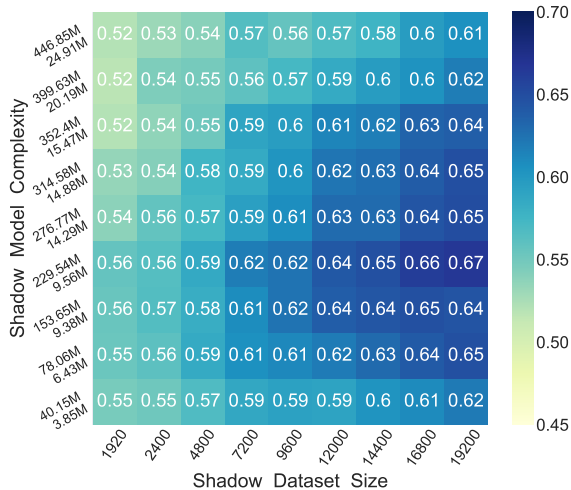


Fig. 3: Attack AUC under the effect of changing the dataset size and shadow model complexity (upper is the number of parameters, lower is the computational complexity FLOPs). The target model (\mathcal{M} -2, CIFAR-10)’s training set size is 9600, and complexity is 229.54M parameters and 9.56M FLOPs.

- Higher similarity between the shadow model and the target model leads to better attack performance.
- Even simpler shadow models (one-third of the parameters, one-fifth of the computational complexity, or less) can achieve strong attack performance.

In addition, we experiment with other statistical metrics, including the maximal posterior and entropy, for our attack. Figure 2 shows AUC on the MNIST, CIFAR-10, and CIFAR-100 datasets, the results for other datasets can be found in the Appendix. We can observe that loss achieves the highest performance with respect to different overfitting levels. Meanwhile, the AUC score is almost the same for maximal posterior and entropy. This indicates the loss value contains the strongest signal on differentiating member and non-member samples.

Figure 4 further shows the loss distribution of member and

non-member samples from the target model calculated on the shadow model (\mathcal{M} -0 and \mathcal{M} -5 on CIFAR-10 and CIFAR-100, results for other datasets are listed in the Appendix). Though both member and non-member samples are never used to train the shadow model, we still observe a clear difference between their loss. This verifies our **Proposition 1** in Section III-B: If the shadow model and the target model are similar enough, a member sample from the target model can also receive a confident prediction by the shadow model.

IV. PERTURBATION-BASED MEMBERSHIP INFERENCE ATTACK

After demonstrating the effectiveness of our transfer-based membership inference attack, we now present our second attack, i.e., perturbation-based membership inference. We start with the threat model description. Then, we introduce the attack methodology. In the end, we present the evaluation results.

A. Threat Model

Compared to the transfer-based attack, our perturbation-based attack has minimal assumption. This indicates the adversary does not have a shadow dataset to train a shadow model. All she could rely on is the predicted label for the target sample from the target model. To the best of our knowledge, this is by far the most strict setting for membership inference against machine learning classifiers.

B. Key Intuition

Our intuition behind this attack follows a general observation of the overfitting nature of ML models. Specifically, an ML model is more confident in predicting samples that it is trained on. In contrast to the previous posterior-based attacks [46], [48] that directly use posteriors as inputs, we place our focus on the antithesis of this observation, i.e., since the ML model is more confident on member data samples, it should be much harder to change its mind.

Figure 5 depicts the posteriors for two randomly selected member data samples (Figure 5a, Figure 5c) and non-member

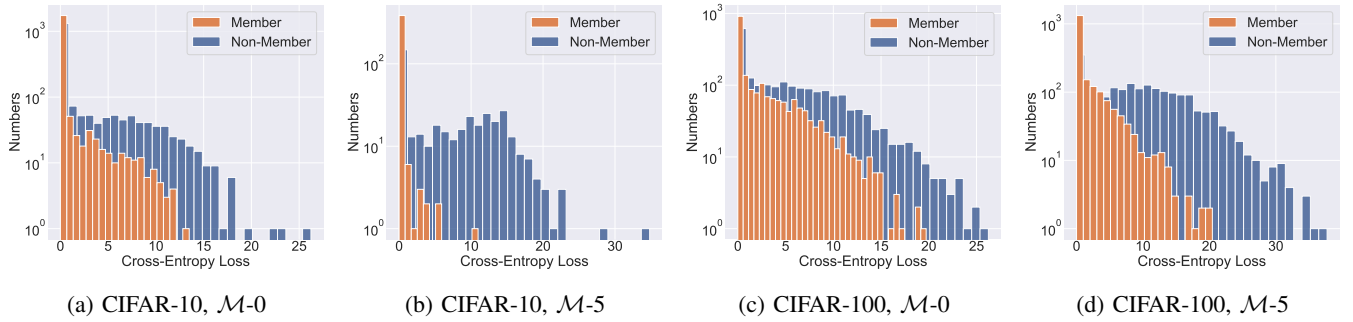


Fig. 4: The cross entropy loss distribution obtained from the shadow model. The x-axis represents the loss value and the y-axis represents the number of the loss.

TABLE III: The cross entropy between the target model’s output posterior and other labels except for the predicted label. ACE represent the average cross entropy.

Status	Ground Truth Label	Predicted Label	0	1	2	3	Cross Entropy		6	7	8	9	ACE
							4	5					
(a) Member	6	6	7.8156	8.3803	4.1979	1.0942	4.1367	4.3492	-	7.6328	1.5522	1.2923	4.4946
(b) Non-member	8	8	2.3274	0.8761	0.8239	2.0793	1.2275	0.9791	1.2373	1.1152	-	5.0451	1.2218
(c) Member	3	3	1.2995	5.2842	5.4212	-	1.5130	4.8059	4.5897	7.1547	3.2411	4.7910	4.2334
(d) Non-member	7	9	2.8686	1.8325	3.6480	0.5352	1.8722	1.1689	4.0124	0.6866	3.1071	-	2.1766

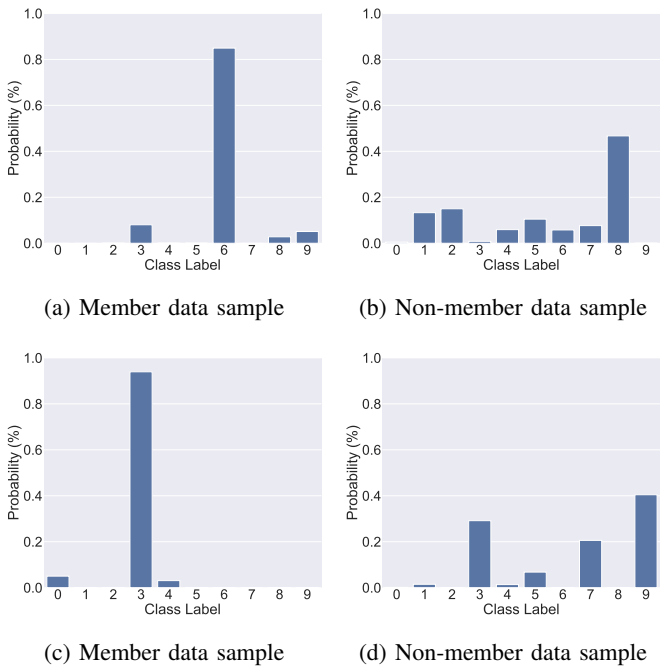


Fig. 5: The posterior probability distribution of the target model (\mathcal{M} -0, CIFAR-10) on two member data samples and two non-member data samples.

data samples (Figure 5b, Figure 5d) with respect to \mathcal{M} -0 trained on CIFAR-10. We can observe that the maximal posterior for member samples is indeed much higher than the one of non-member samples. We further use cross entropy, a common metric for classification task, to quantify the difficulty

for an ML model to change its predicted label for a data sample to other labels.

$$CE = - \sum_{i=0}^K \mathcal{Y}_i \log(\mathcal{M}_i(x))$$

Here, $\mathcal{Y}_i \in \{0, 1\}$ is i -th class vector of the one-hot encoding label except for the predicted label and K is the number of classes (see Section II). Table III shows the cross entropy between posteriors and other labels for these two member and two non-member samples. We can see that member samples cross entropy is significantly larger than non-member samples. These observation leads to the following proposition.

Proposition 2. Given an ML model and a set of data samples, the cost for changing member samples’ predicted labels is larger than that for non-member samples.

Furthermore, consider an ML model which only provides predicted labels instead of posteriors, we have the following proposition.

Proposition 3. When using adversarial perturbation to change predicted labels of an ML model for a set of data samples, the noise added to member samples is larger than that to non-member samples.

Following this proposition, we propose to use the magnitude of the perturbation on a sample to determine whether the sample is a member or not.

C. Methodology

Our attack methodology consists of the following three stages, i.e., perturbation generation, noise measurement, and membership inference.

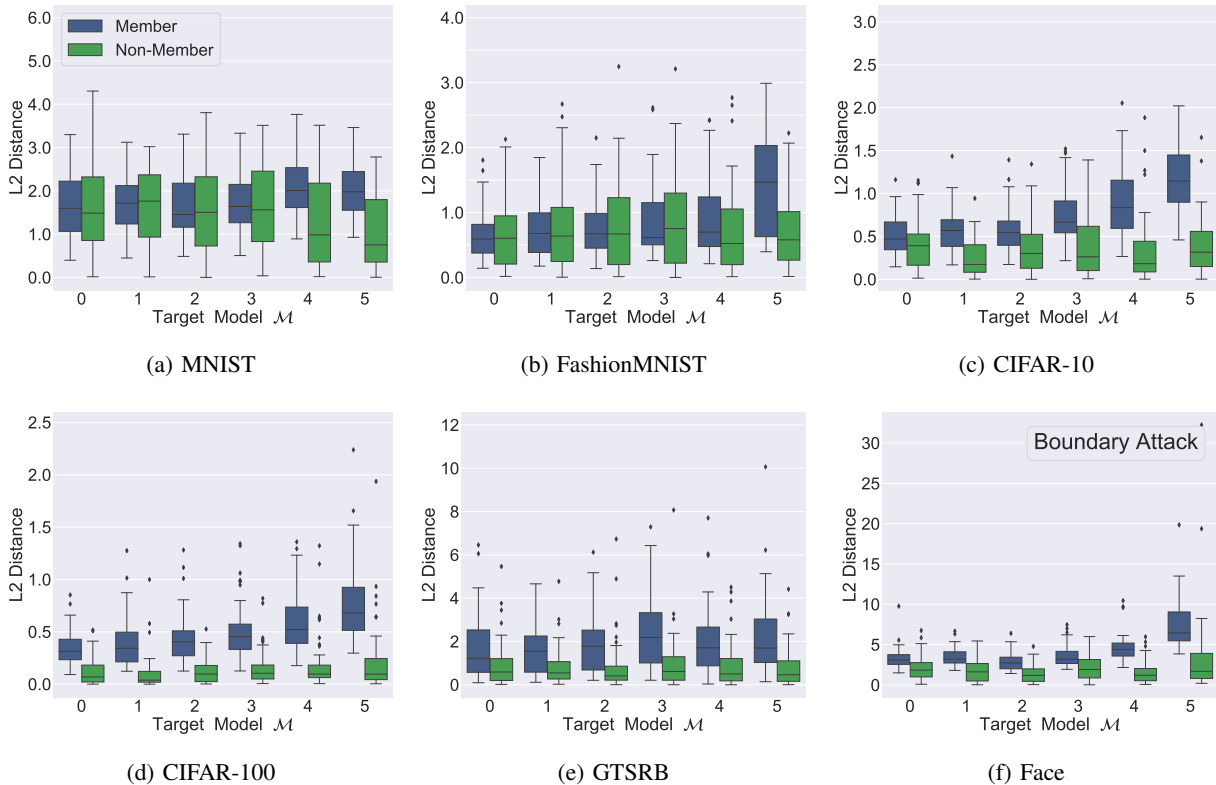


Fig. 6: L_2 distance between the original sample and its perturbed samples generated by the Boundary attack. The x-axis represents the target model being attacked and the y-axis represents the L_2 distance.

Perturbation Generation. The goal of changing the predicted label is similar to that of adversarial examples [9], [12], [39], [40], [47], [51], thus we use the same technique to modify the input to mislead the target model. As the adversary only has black-box access to the target ML model, we adopt untargeted black-box adversarial attacks, such as Boundary [10], SaltAndPepperNoise [6], and AdditiveUniformNoise [6] in our attack.

Noise Measurement. Once the perturbation has finished, we measure the magnitude of the noise added to the target sample. In general, adversarial attacks typically use L_p distance (or Minkowski Distance), e.g., L_0 , L_1 , L_2 , and L_∞ , to measure the perceptual similarity between a perturbed sample and its original one. Thus, the adversary can also use L_p distance to measure the noise.

Membership Inference. After obtaining the magnitude of the noise, the adversary simply considers a sample with noise larger than a threshold as a member sample, and vice versa. Similar to the transfer-based attack, we mainly use AUC as our evaluation metric. We also provide a general and simple method for choosing a threshold in Section V.

D. Evaluation

Experiment Setup. We use the same experiment setup as presented in Section III, such as the dataset splitting strategy and

training 6 target models with different overfitting levels. We perform our attack over all datasets. For evaluation metric, we again adopt AUC. Regarding perturbation generation, we use the source code provided by Foolbox [6]. For space reasons, we report the results of Boundary and SaltAndPepperNoise in the main body of the paper. Results by AdditiveUniformNoise can be found in the Appendix.

Results. First, we show the distribution of noise between a perturbed sample and its original one for member and non-member samples in Figure 6 and Figure 7. Both Boundary and SaltAndPepperNoise attacks apply L_2 distance to limit the magnitude of perturbation, thus we report results of L_2 distance as well. As expected, the magnitude of the perturbation on member samples is indeed larger than that on non-member samples. For instance in Figure 6 (\mathcal{M} -5, CIFAR-10), the average L_2 distance of the perturbation for member samples is 1.2282, while that for non-member samples is 0.6624. In addition, models with lower overfitting level require less perturbation. As the overfitting level increases, the adversary needs to modify more on the given sample. The reason is that an ML model with a higher overfitting level has remembered its training samples to a larger extent, thus it is much harder to change their predicted labels, i.e., larger perturbation is required.

We report the AUC values over all dataset in Figure 8 and Figure 9. We compare 4 different distance metrics, i.e., L_0 , L_1 , L_2 , and L_∞ , for each perturbation scheme. For the

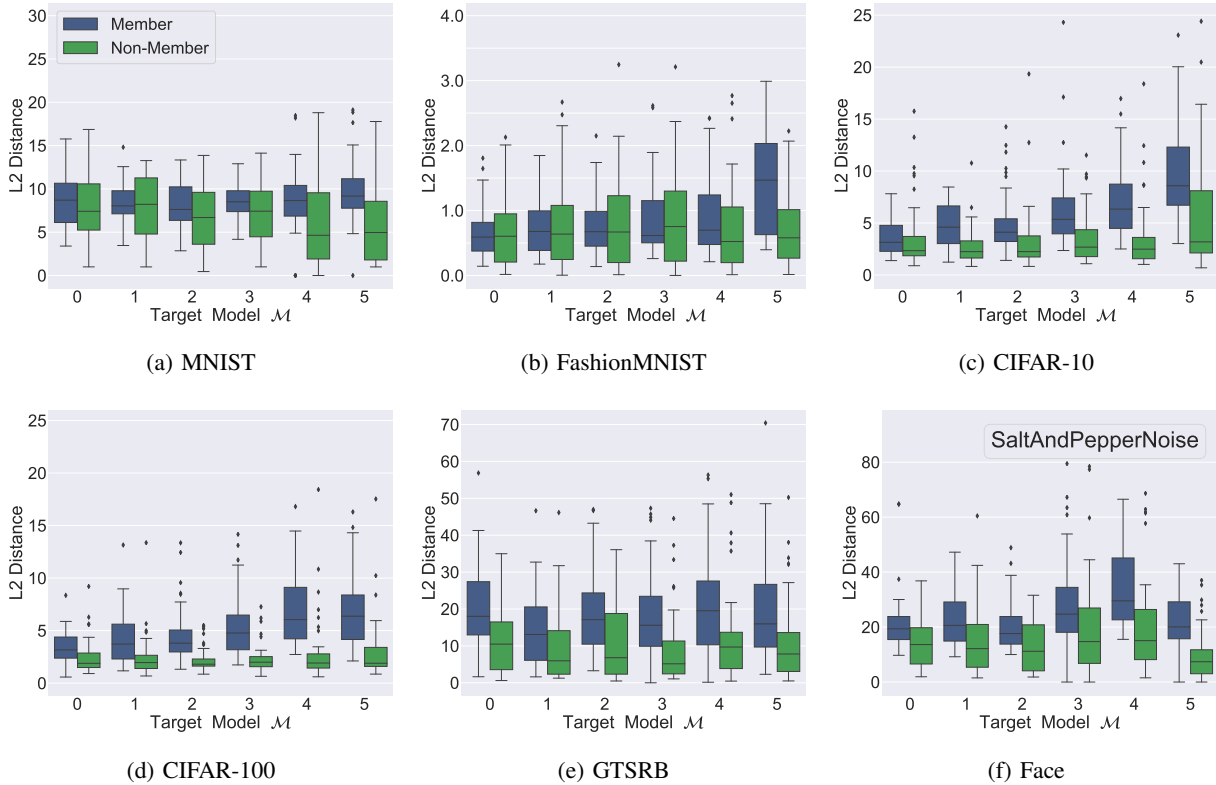


Fig. 7: L_2 distance between the original sample and its perturbed samples generated by the SaltAndPepperNoise attack. The x-axis represents the target model being attacked and the y-axis represents the L_2 distance.

Boundary attack in Figure 8, we can observe that L_1 distance and L_2 distance achieve the best performance followed by L_∞ distance across all datasets. L_0 distance performs the worst. For instance, on the CIFAR-10 dataset with \mathcal{M} -5, the AUC scores for L_1 distance, L_2 distance, and L_∞ distance are 0.9188, 0.9216, and 0.9164, respectively, while the AUC score for L_0 distance is 0.6132. It is worth noting that other metrics, including L_1 and L_∞ , can also achieve similar performance for the Boundary attack. In contrast, for the SaltAndPepperNoise attack in Figure 9, the AUC score of the L_0 distance achieves the best performance, followed by the L_1 distance and L_2 distance. This provides the adversary with some guidelines on how to choose perturbation generation approaches and distance measurement metrics.

All the above results have sufficiently demonstrated the efficacy of our proposed perturbation-based attack. Next, we take a deeper look on why this attack works.

First, we study the decision boundary of the target model (CIFAR-10, \mathcal{M} -4) with a given set of data samples, including 800 member samples and 800 non-member samples. To better visualize the decision boundary, there are two points to note:

- The adversary can only rely on the predicted label, so it is difficult to gain insight from the original input space which is connected with the ground truth label. Thus we visualize the decision boundary of the transformed space, i.e., the output space of the last hidden layer which is fully connected with the

predicted label space.

- Due to the limitations of the target dataset size, we further sample a large number of random samples across the output space so that we can fill the whole space, which can clearly visualize the decision boundary that distinguishes between different predicted labels.

To this end, we map the given data samples into the transformed space and embed the output posteriors into a 2D space using t-Distributed Stochastic Neighbor Embedding (t-SNE). Figure 10a shows the results for 10 classes of CIFAR-10. We can see that the given data samples have been clearly classified into 10 classes and mapped to 10 different regions. For the sake of analysis, we purposely zoom in three different regions in the upper left of the whole space. As we can see in Figure 10b, the member samples and non-member samples belonging to the same predicted label are tightly divided into 2 clusters, which explains why the previous posterior-based attack can achieve effective performance. More interestingly, we can see that the member samples are further away from the decision boundary than the non-member samples, that is, the distance between the members and the decision boundary is larger than that of the non-members. Again, this validates our key intuition.

Recall that in the first stage, we apply black-box adversarial attacks for perturbation generation. Here, we give an intuitive overview of how the Boundary attack and SaltAndPepperNoise attack work in Figure 10c. As we can see, though these two attacks adopt different strategies to find the perturbed

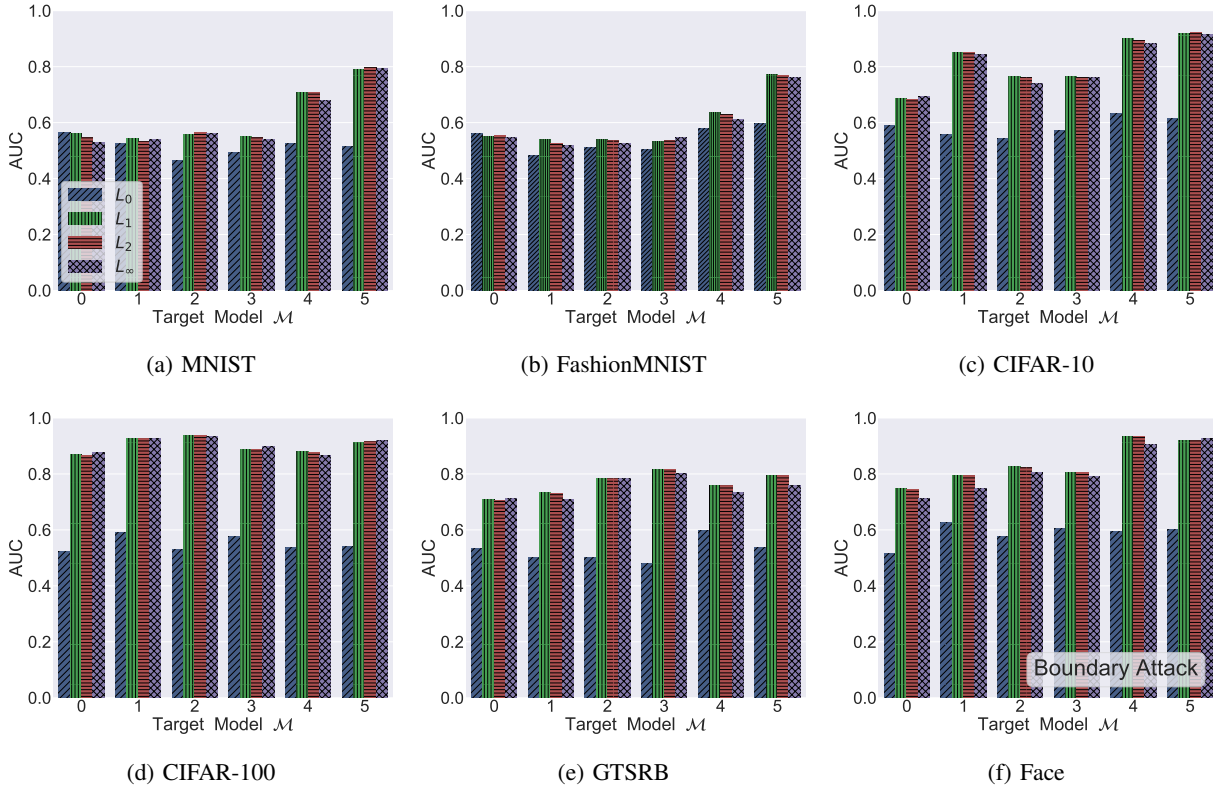


Fig. 8: Attack AUC for four different L_p distances to measure the distance between the original samples and its perturbed samples generated by the Boundary attack. The x-axis represents the target model being attacked and the y-axis represents the AUC score.

sample, there is one thing in common: The search ends at the tangent points between the neighboring L_p -radius ball of the original sample and its decision boundary. Only in this way they can mislead the target model and also generate a small perturbation. Combined with Figure 10b, we can find that the magnitude of perturbation is essentially a reflection of the distance from the original sample to its decision boundary. Quantitatively, in the following, we verify whether the distance from member samples to its decision boundary is larger than non-member samples.

E. Certified Radius

We investigate the relationship between the membership status of samples and their neighboring L_p -radius ball in a classification task. This neighboring L_p -radius ball, which reflects the magnitude of perturbation, is also called the *Robust Radius*. It is defined as the L_p robustness of the target model at a data sample and it represents the radius of the largest L_p ball centered at the data sample in which the target model does not change its prediction, as shown in Figure 10c. In this work, we investigate the L_2 robustness of the target model \mathcal{M} at a data sample x . As previous work [55] shows that computing the L_2 robust radius of a model is NP-hard, similar to Zhai et al. [58], we also derive a tight lower bound of Robust Radius, namely *Certified Radius*, which satisfies $0 \leq CR(\mathcal{M}; x, y) \leq R(\mathcal{M}; x, y)$ for any \mathcal{M}, x and corresponding label $y \in \{1, 2, \dots, K\}$. Note that, we use $f_{\mathcal{M}}$

represents the target model’s predicted label in the following, where $\mathcal{M}(x)$ represents the target model’s posteriors.

Randomized Smoothing. In this work, we apply a recent technique, called randomized smoothing [17], which is scalable to any architectures, to obtain the certified radius of smoothed deep neural networks. The key part of randomized smoothing is to use the smoothed version of \mathcal{M} , which is denoted by \mathcal{G} , to make predictions. The formulation of \mathcal{G} is defined as follows.

Definition 1. For an arbitrary classifier \mathcal{M} and $\sigma > 0$, the smoothed classifier \mathcal{G} of \mathcal{M} is defined as

$$f_{\mathcal{G}}(x) = \arg \max_{c \in \mathcal{Y}} P_{\varepsilon \sim \mathcal{N}(0, \sigma^2 \mathbf{I})} (f_{\mathcal{M}}(x + \varepsilon) = c) \quad (1)$$

In short, the smoothed classifier \mathcal{G} returns the label most likely to be returned by \mathcal{M} when its input is sampled from a Gaussian distribution $\mathcal{N}(x, \sigma^2 \mathbf{I})$ centered at x . Cohen et al. [17] prove the following theorem, which provides an analytic form of certified radius:

Theorem 1. [17] Let $f_{\mathcal{M}} : x \rightarrow y$, and $\varepsilon \sim \mathcal{N}(0, \sigma^2 \mathbf{I})$. Let the smoothed classifier \mathcal{G} be defined as in (1). Let the ground truth of an input x be its prediction y . If \mathcal{G} classifies x correctly, i.e.,

$$P_{\varepsilon}(f_{\mathcal{M}}(x + \varepsilon) = y) \geq \max_{y' \neq y} P_{\varepsilon}(f_{\mathcal{M}}(x + \varepsilon) = y') \quad (2)$$

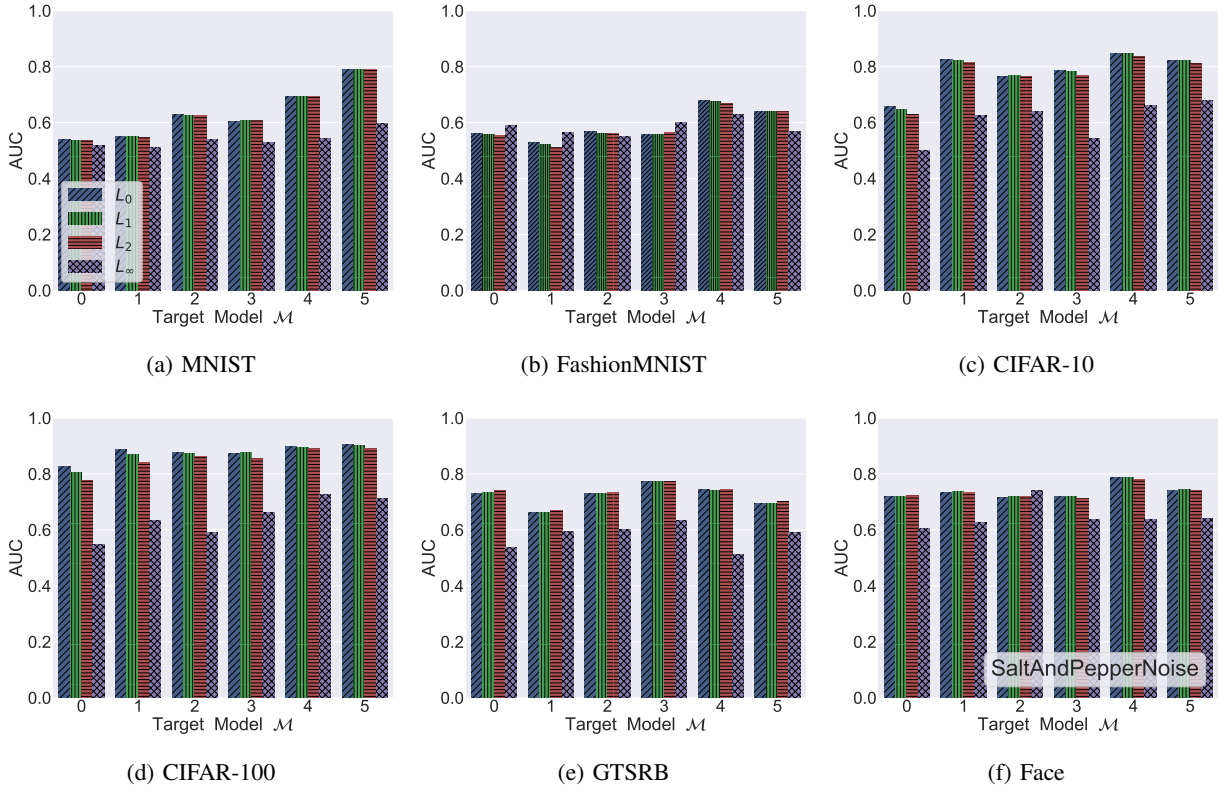


Fig. 9: Attack AUC for four different L_p distances to measure the distance between the original sample and its perturbed samples generated by the SaltAndPepperNoise attack. The x-axis represents the target model being attacked and the y-axis represents the AUC score.

Then \mathcal{G} is provably robust at x , with the certified radius given by

$$\begin{aligned}
 CR(f_{\mathcal{G}}; x, y) &= \frac{\sigma}{2} [\Phi^{-1}(P_{\varepsilon}(f_{\mathcal{M}}(x + \varepsilon) = y)) \\
 &\quad - \Phi^{-1}(\max_{y' \neq y} P_{\varepsilon}(f_{\mathcal{M}}(x + \varepsilon) = y'))] \\
 &= \frac{\sigma}{2} [\Phi^{-1}(\mathbb{E}_{\varepsilon} \mathbf{1}_{\{f_{\mathcal{M}}(x + \varepsilon) = y\}}) \\
 &\quad - \Phi^{-1}(\max_{y' \neq y} \mathbb{E}_{\varepsilon} \mathbf{1}_{\{f_{\mathcal{M}}(x + \varepsilon) = y'\}})] \quad (3)
 \end{aligned}$$

where Φ is the c.d.f. of the standard Gaussian distribution.

ACR of Members and Non-members. For the target model \mathcal{M} and each data sample $(x, f_{\mathcal{M}}(x))$, we can estimate the certified radius $CR(\mathcal{M}; x, f_{\mathcal{M}}(x))$. Here, we use the *average certified radius* (ACR) as a metric.

We report the results on target models with different overfitting levels over all datasets. From the results summarized in Table IV, we can draw the following conclusions.

- The ACR of member samples is universally greater than the ACR of non-member samples, which forms the basis for the success of our perturbation-based attack.
- The difference between the ACR of member samples and non-member samples also increases with the in-

creasing overfitting level, which exactly reflects the increasing attack performance in the aforementioned AUC results.

The key to the success of our perturbation-based attack is the difference between member’s CR and non-member’s CR , and this difference can be exactly reflected in the adversarial perturbation against the robustness. Note that almost all certified radius is to certify the robustness of an ML model, in this paper, we are the first to use it to certify the privacy of an ML model. We believe that this leaves an interesting direction for future research into robustness and privacy in classification.

V. DISCUSSIONS

Comparison of Different Attacks. Figure 11 compares the performance of the attack by Salem et al. [48] and our 2 attacks. In particular, we show the best performance for our second attack by adopting the Boundary method for perturbation generation. As we can see, our perturbation-based attack achieves the best performance for most of the datasets except for GTSRB. As our perturbation-based attack exploits the least information, i.e., predicted labels, to mount the attack, this demonstrates the efficacy of our proposed label-only membership inference attack, thereby the corresponding membership privacy risks stemming from ML models are much more severe than previously shown.

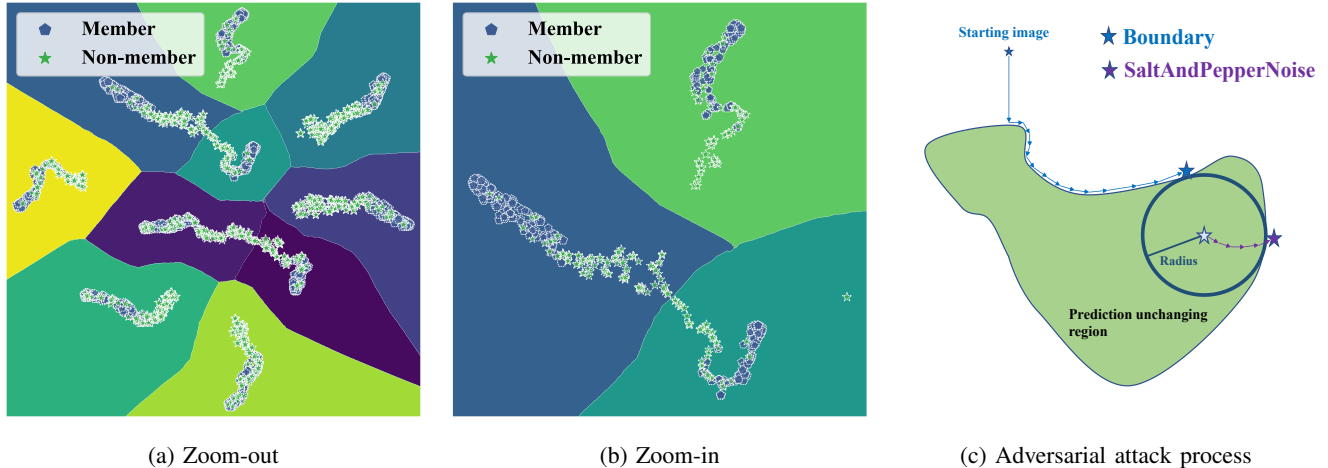


Fig. 10: Decision regions of different predicted labels (a)(b), and the search process of perturbed sample by the Boundary attack and SaltAndPepperNoise Attack (c).

TABLE IV: Average certified radius (ACR) of members and non-members across all target models and datasets.

Target Model	MNIST		FashionMNIST		CIFAR-10		CIFAR-100		GTSRB		Face	
	Member	Non-mem	Member	Non-mem	Member	Non-mem	Member	Non-mem	Member	Non-mem	Member	Non-mem
\mathcal{M} -0	0.8704	0.7780	0.4605	0.3826	0.1636	0.1633	0.0292	0.0198	0.4667	0.3232	0.0638	0.0614
\mathcal{M} -1	0.8876	0.8001	0.5115	0.3861	0.2166	0.1203	0.0447	0.0318	0.4648	0.2815	0.2172	0.1332
\mathcal{M} -2	0.8943	0.7047	0.5497	0.4142	0.2245	0.1459	0.0401	0.0082	0.4274	0.2391	0.1708	0.1494
\mathcal{M} -3	0.8982	0.6866	0.5783	0.4347	0.3573	0.2029	0.1086	0.0304	0.4497	0.1936	0.1306	0.1475
\mathcal{M} -4	0.9215	0.6146	0.6283	0.3816	0.4191	0.1980	0.1695	0.0281	0.4659	0.1973	0.3049	0.3382
\mathcal{M} -5	0.9143	0.5175	0.7350	0.3312	0.5167	0.3239	0.2876	0.0599	0.4262	0.2245	0.2668	0.4287

Threshold Choosing. As mentioned before, in the membership inference stage for both of our attacks, the adversary needs to make a manual decision on what threshold to use. For the transfer-based attack, since we assume that the adversary has a dataset that comes from the same distribution as the target models training set, she can rely on the shadow dataset to estimate a threshold by sampling certain part of that dataset as non-member samples.

Here, we mainly focus on our perturbation-based attack where the adversary is not equipped with a shadow dataset. We provide a simple and general method for choosing a threshold. Concretely, we generate a set of random samples in the feature space as the target model’s training set. In the case of image classification, we sample each pixel for an image from a uniform distribution. Next, we treat these randomly generated samples as non-members and query them to the target model. Then, we add adversarial perturbations on these random samples to change their initial predicted labels by the target model. In the end, we use these samples’ magnitude of perturbation to estimate a threshold, i.e., finding a suitable top t percentile over these perturbation.

We experimentally generate 100 random samples for \mathcal{M} -5 trained with CIFAR-10 and CIFAR-100, respectively, and adopt the Boundary attack for perturbation generation. We again use the L_2 distance to measure the magnitude of perturbation and F1 score as our evaluation metric. Figure 12 shows the results over different t . As we can see, setting t from 5 to 40 achieves a good performance for both cases. In

addition, even the worse performance when $t=90$ is still quite good (0.7092 for CIFAR-10 and 0.6803 for CIFAR-100). Thus, we conclude that our threshold-choosing method can achieve good performance.

Query Limitation. To mount our perturbation-based attacks in the real-world ML application, such as Machine Learning as a Service (MLaaS), the adversary cannot issue as many queries as she wants, since a large number of queries increases the cost of the attack and may cause suspicion of the model provider. We now evaluate the attack performance with different number of queries. Here, we also adopt the Boundary attack for perturbation generation on CIFAR-10 and CIFAR-100 datasets. We vary the number of queries from 0 to 20,000, and evaluate the attack performance based on the L_2 distance. As we can see in Figure 13, the AUC increases sharply with the increase of the number of queries in the beginning. For instance, when querying 10 times, the AUC for CIFAR-10 is 0.6928 and CIFAR-100 is 0.8060. At this time, though the perturbed sample is far away from its origin’s decision boundary, the magnitude of perturbation for member samples is still relatively larger than that for non-member samples. After 3,000 queries, the attack performance becomes stable. In the future, we plan to investigate means to reduce the number of queries.

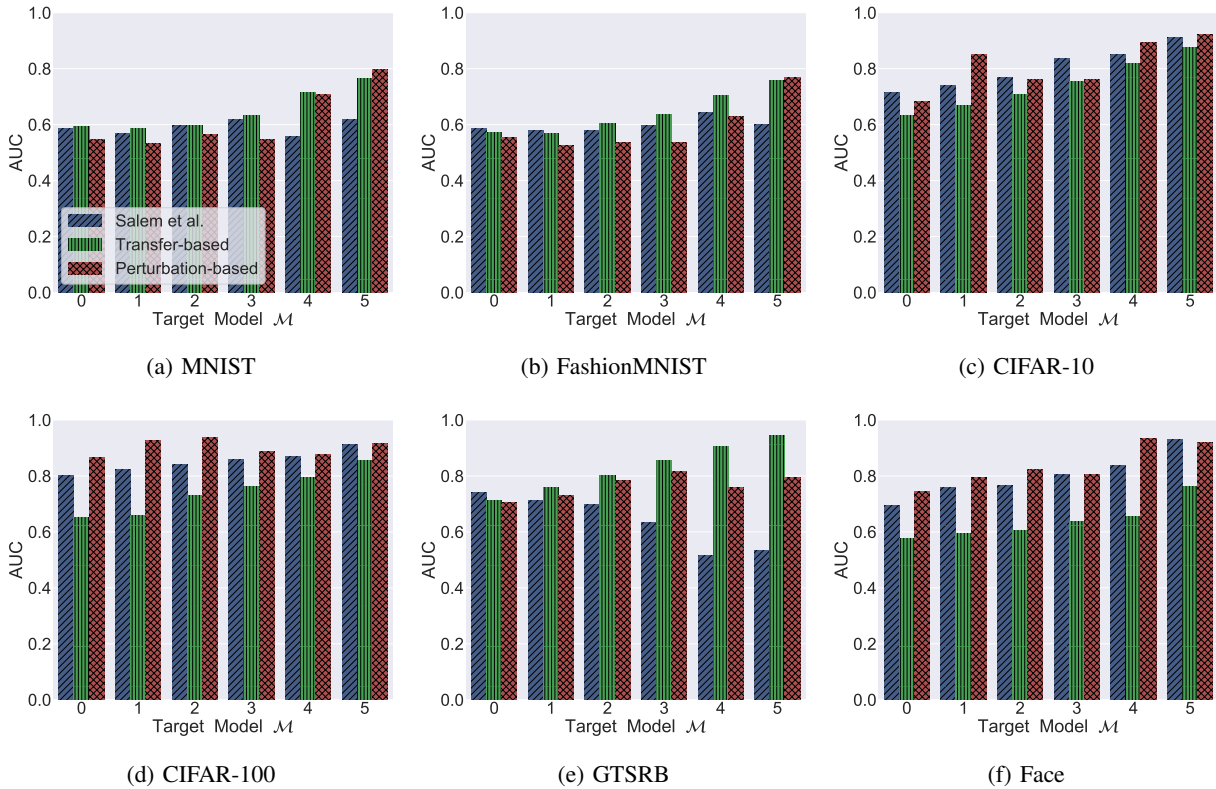


Fig. 11: Comparison of our transfer-based and perturbed-based performance with the attack by Salem et al. across all target models. The x-axis represents the target model being attacked and the y-axis represents the AUC score.

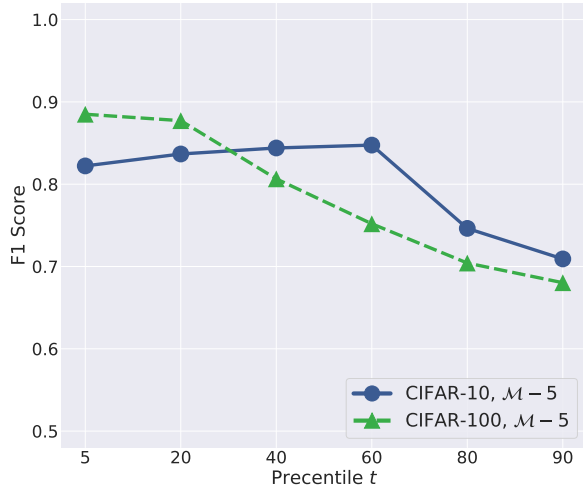


Fig. 12: The relation between the percentile of the L_2 distance, i.e., threshold, and perturbation-based attacks performance. The x-axis represents the percentile t and the y-axis represents the F1 score.

VI. RELATED WORKS

Membership Inference Against Machine Learning. Membership inference attack has been successfully performed in

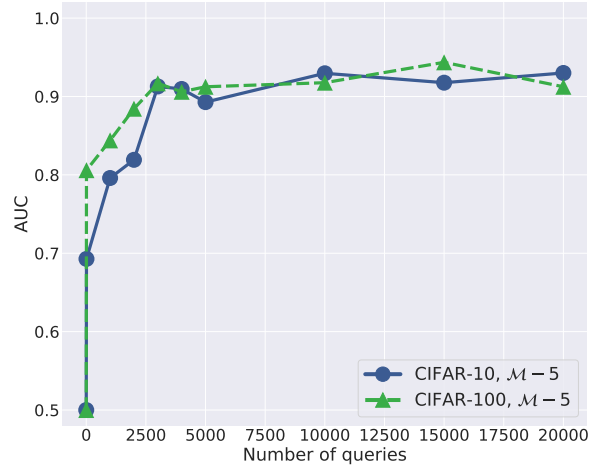


Fig. 13: Attack AUC under the effect of number of queries. The x-axis represents the number of queries and the y-axis represents the AUC score for perturbation-based attack.

various data domains, ranging from biomedical data [7], [22], [26] to mobility traces [41]. Shokri et al. [48] present the first membership inference attack against machine learning models. The general idea behind is to use multiple shadow models to generate data to train multiple attacks models (one for each class). These attack models take the target sample’s posteriors

as input. Salem et al. [46] later present another attack by gradually relaxing the assumptions made by Shokri et al. [48] achieving a model and data independent membership inference. Yeom et al. [57] quantitatively analyze the relationship between the attacks and the loss over both training set and testing set and propose a general attack. Long et al. [32] proposes an indirect attack by analyzing the distribution of the perturbed sample’s posteriors. Besides classifiers, others have performed membership inference attacks against other types of ML models [13], [23], [29], [33], [35], [49].

As pointed out before, all these attacks are posterior-based. In this work, we study label-only membership inference attack. Prior to this, multiple works have performed initial investigation on label-only membership inference [25], [42], [57]. We also acknowledge that there is a concurrent work which proposes a similar approach as our perturbation-based attack [16]. Besides, we further introduce a novel transfer-based attack in this paper.

Multiple defense mechanisms have been proposed to mitigate membership privacy risks. As overfitting is the major reason for membership inference to be successful, several approaches have been proposed with the aim of reducing overfitting [34], [46], [48]. Recently, Jia et al. [27] introduce MemGuard, the first defense with formal utility-loss guarantees against black-box membership inference attacks. The basic idea behind this work is to add carefully crafted noise to posteriors of an ML model to mislead the membership classifier. Yang et al. [56] also propose a similar defense in this direction. One common utility requirement adopted by these methods is that the predicted label for a sample cannot be changed. This however indicates that they cannot be used to mitigate our label-only attack.

Other Attacks Against Machine Learning. In recent years, there are many other attacks against ML models [38]. One major attack in the field is adversarial examples [9], [12], [39], [40], [47], [51], we leverage its technique to establish our perturbation-based attack. Meanwhile, backdoor attacks have received a lot of attention [15], [21], [30], [31], [45], [50], [54]. Ganju et al. [20] propose a property inference attack aiming at to infer general properties of the target model’s training set, such as training samples’ gender distribution. Salem et al. [44] study the problem of dataset reconstruction in the online learning setting by proposing a novel generative adversarial network model. Tramèr et al. [52] present the first attack on stealing an ML classifier’s parameters. Recently, Krishna et al. [28] extend the model stealing attack to natural language processing models. Besides model parameters, other works focus on stealing the target model’s hyperparameters [36], [53].

VII. CONCLUSION

During the past decade, machine learning has made rapid progress. Nowadays, ML models have been deployed in various real-world applications, such as image recognition and machine translation. However, recent research shows that ML models are vulnerable to various attacks against its training set [11], [14], [18]–[20], [24], [33], [37], [43], [44], [46], [48]. One major attack in this field is membership inference where

the adversary aims to determine whether a data sample is part of the target ML model’s training set.

The current membership inference attacks mainly leverage the overfitting behavior of an ML model. That is an ML model is more confident in its prediction for a training/member sample, and this confidence is reflected on the model’s output, i.e., posteriors. Therefore, all the current attacks leverage posteriors as inputs to achieve effective performance. However, these attacks can be trivially mitigated if the target model only returns the predicted label instead of posteriors.

In this paper, we systematically investigate label-only membership inference attack to examine whether a predicted label alone can leak the corresponding target sample’s membership status. We propose two attacks tailored for two threat models, namely transfer-based attack and perturbation-based attack. For the transfer-based attack, we assume the adversary has a shadow dataset (without labels) that comes from the same distribution as the target model’s training set. Then, she uses the target model as an oracle to label her shadow dataset and trains a shadow model based on it. In the end, to mount the attack, the adversary calculates the prediction confidence of the target sample with respect to the shadow model and make her prediction with the confidence. Our transfer-based attack follows the intuition that if the shadow model and the target model are similar enough, then a member sample of the target model should also receives confident prediction by the shadow model.

For the perturbation-based attack, the adversary is not equipped with a shadow dataset. In this case, the attack’s intuition is that it is harder to perturb a member sample to a different class than a non-member sample. To this end, the adversary utilizes the technique of adversarial example to add perturbation to the target sample and judges the sample’s membership status based on the magnitude of the perturbation.

We have performed extensive experiments over a set of 6 datasets. Evaluation results show that both of our attacks achieve effective performance. Our work demonstrates the severity of membership privacy risks stemming from machine learning models, and we believe it can serve as a stepping stone for more advanced attacks and effective defense mechanisms in the future.

REFERENCES

- [1] <https://www.cs.toronto.edu/~kriz/cifar.html>. 1, 2
- [2] <http://yann.lecun.com/exdb/mnist/>. 2
- [3] <https://research.zalando.com/welcome/mission/research-projects/fashion-mnist/>. 2
- [4] <http://benchmark.ini.rub.de/?section=gtsrb>. 2
- [5] <http://vis-www.cs.umass.edu/lfw/>. 2
- [6] <https://github.com/bethgelab/foolbox>. 7
- [7] M. Backes, P. Berrang, M. Humbert, and P. Manoharan, “Membership Privacy in MicroRNA-based Studies,” in *ACM SIGSAC Conference on Computer and Communications Security (CCS)*. ACM, 2016, pp. 319–330. 12
- [8] M. Backes, M. Humbert, J. Pang, and Y. Zhang, “walk2friends: Inferring Social Links from Mobility Profiles,” in *ACM SIGSAC Conference on Computer and Communications Security (CCS)*. ACM, 2017, pp. 1943–1957. 4

- [9] B. Biggio, I. Corona, D. Maiorca, B. Nelson, N. Srndic, P. Laskov, G. Giacinto, and F. Roli, "Evasion Attacks against Machine Learning at Test Time," in *European Conference on Machine Learning and Principles and Practice of Knowledge Discovery in Databases (ECML/PKDD)*. Springer, 2013, pp. 387–402. 7, 13
- [10] W. Brendel, J. Rauber, and M. Bethge, "Decision-Based Adversarial Attacks: Reliable Attacks Against Black-Box Machine Learning Models," in *International Conference on Learning Representations (ICLR)*, 2018. 7
- [11] N. Carlini, C. Liu, Ú. Erlingsson, J. Kos, and D. Song, "The Secret Sharer: Evaluating and Testing Unintended Memorization in Neural Networks," in *USENIX Security Symposium (USENIX Security)*. USENIX, 2019, pp. 267–284. 1, 13
- [12] N. Carlini and D. Wagner, "Towards Evaluating the Robustness of Neural Networks," in *IEEE Symposium on Security and Privacy (S&P)*. IEEE, 2017, pp. 39–57. 7, 13
- [13] D. Chen, N. Yu, Y. Zhang, and M. Fritz, "GAN-Leaks: A Taxonomy of Membership Inference Attacks against GANs," in *ACM SIGSAC Conference on Computer and Communications Security (CCS)*. ACM, 2020. 13
- [14] M. Chen, Z. Zhang, T. Wang, M. Backes, M. Humbert, and Y. Zhang, "When Machine Unlearning Jeopardizes Privacy," CoRR abs/2005.02205, 2020. 1, 13
- [15] X. Chen, A. Salem, M. Backes, S. Ma, and Y. Zhang, "BadNL: Backdoor Attacks Against NLP Models," CoRR abs/2006.01043, 2020. 13
- [16] C. A. C. Choo, F. Tramer, N. Carlini, and N. Papernot, "Label-Only Membership Inference Attacks," CoRR abs/2007.14321, 2020. 13
- [17] J. M. Cohen, E. Rosenfeld, and J. Z. Kolter, "Certified Adversarial Robustness via Randomized Smoothing," in *International Conference on Machine Learning (ICML)*. JMLR, 2019, pp. 1310–1320. 9
- [18] M. Fredrikson, S. Jha, and T. Ristenpart, "Model Inversion Attacks that Exploit Confidence Information and Basic Countermeasures," in *ACM SIGSAC Conference on Computer and Communications Security (CCS)*. ACM, 2015, pp. 1322–1333. 1, 13
- [19] M. Fredrikson, E. Lantz, S. Jha, S. Lin, D. Page, and T. Ristenpart, "Privacy in Pharmacogenetics: An End-to-End Case Study of Personalized Warfarin Dosing," in *USENIX Security Symposium (USENIX Security)*. USENIX, 2014, pp. 17–32. 1, 4, 13
- [20] K. Ganju, Q. Wang, W. Yang, C. A. Gunter, and N. Borisov, "Property Inference Attacks on Fully Connected Neural Networks using Permutation Invariant Representations," in *ACM SIGSAC Conference on Computer and Communications Security (CCS)*. ACM, 2018, pp. 619–633. 1, 13
- [21] T. Gu, B. Dolan-Gavitt, and S. Grag, "Badnets: Identifying Vulnerabilities in the Machine Learning Model Supply Chain," CoRR abs/1708.06733, 2017. 13
- [22] I. Hagestedt, Y. Zhang, M. Humbert, P. Berrang, H. Tang, X. Wang, and M. Backes, "MBeacon: Privacy-Preserving Beacons for DNA Methylation Data," in *Network and Distributed System Security Symposium (NDSS)*. Internet Society, 2019. 4, 12
- [23] J. Hayes, L. Melis, G. Danezis, and E. D. Cristofaro, "LOGAN: Evaluating Privacy Leakage of Generative Models Using Generative Adversarial Networks," *Symposium on Privacy Enhancing Technologies Symposium*, 2019. 13
- [24] X. He, J. Jia, M. Backes, N. Z. Gong, and Y. Zhang, "Stealing Links from Graph Neural Networks," CoRR abs/2005.02131, 2020. 1, 13
- [25] Y. He, S. Rahimian, B. Schiele, and M. Fritz, "Segmentations-Leak: Membership Inference Attacks and Defenses in Semantic Image Segmentation," CoRR abs/1912.09685, 2019. 13
- [26] N. Homer, S. Szelinger, M. Redman, D. Duggan, W. Tembe, J. Muehling, J. V. Pearson, D. A. Stephan, S. F. Nelson, and D. W. Craig, "Resolving Individuals Contributing Trace Amounts of DNA to Highly Complex Mixtures Using High-Density SNP Genotyping Microarrays," *PLOS Genetics*, 2008. 12
- [27] J. Jia, A. Salem, M. Backes, Y. Zhang, and N. Z. Gong, "MemGuard: Defending against Black-Box Membership Inference Attacks via Adversarial Examples," in *ACM SIGSAC Conference on Computer and Communications Security (CCS)*. ACM, 2019, pp. 259–274. 4, 13
- [28] K. Krishna, G. S. Tomar, A. P. Parikh, N. Papernot, and M. Iyyer, "Thieves of Sesame Street: Model Extraction on BERT-based APIs," in *International Conference on Learning Representations (ICLR)*, 2020. 13
- [29] K. Leino and M. Fredrikson, "Stolen Memories: Leveraging Model Memorization for Calibrated White-Box Membership Inference," in *USENIX Security Symposium (USENIX Security)*. USENIX, 2020. 13
- [30] Z. Li, C. Hu, Y. Zhang, and S. Guo, "How to Prove Your Model Belongs to You: A Blind-Watermark based Framework to Protect Intellectual Property of DNN," in *Annual Computer Security Applications Conference (ACSAC)*. ACM, 2019, pp. 126–137. 13
- [31] Y. Liu, S. Ma, Y. Aafer, W.-C. Lee, J. Zhai, W. Wang, and X. Zhang, "Trojaning Attack on Neural Networks," in *Network and Distributed System Security Symposium (NDSS)*. Internet Society, 2019. 13
- [32] Y. Long, V. Bindschaedler, L. Wang, D. Bu, X. Wang, H. Tang, C. A. Gunter, and K. Chen, "Understanding Membership Inferences on Well-Generalized Learning Models," CoRR abs/1802.04889, 2018. 1, 2, 13
- [33] L. Melis, C. Song, E. D. Cristofaro, and V. Shmatikov, "Exploiting Unintended Feature Leakage in Collaborative Learning," in *IEEE Symposium on Security and Privacy (S&P)*. IEEE, 2019, pp. 497–512. 1, 13
- [34] M. Nasr, R. Shokri, and A. Houmansadr, "Machine Learning with Membership Privacy using Adversarial Regularization," in *ACM SIGSAC Conference on Computer and Communications Security (CCS)*. ACM, 2018, pp. 634–646. 2, 13
- [35] —, "Comprehensive Privacy Analysis of Deep Learning: Passive and Active White-box Inference Attacks against Centralized and Federated Learning," in *IEEE Symposium on Security and Privacy (S&P)*. IEEE, 2019, pp. 1021–1035. 2, 13
- [36] S. J. Oh, M. Augustin, B. Schiele, and M. Fritz, "Towards Reverse-Engineering Black-Box Neural Networks," in *International Conference on Learning Representations (ICLR)*, 2018. 13
- [37] X. Pan, M. Zhang, S. Ji, and M. Yang, "Privacy Risks of General-Purpose Language Models," in *IEEE Symposium on Security and Privacy (S&P)*. IEEE, 2020, pp. 1471–1488. 1, 13
- [38] N. Papernot, P. McDaniel, A. Sinha, and M. Wellman, "SoK: Towards the Science of Security and Privacy in Machine Learning," in *IEEE European Symposium on Security and Privacy (Euro S&P)*. IEEE, 2018, pp. 399–414. 13
- [39] N. Papernot, P. D. McDaniel, I. Goodfellow, S. Jha, Z. B. Celik, and A. Swami, "Practical Black-Box Attacks Against Machine Learning," in *ACM Asia Conference on Computer and Communications Security (ASIACCS)*. ACM, 2017, pp. 506–519. 7, 13
- [40] N. Papernot, P. D. McDaniel, S. Jha, M. Fredrikson, Z. B. Celik, and A. Swami, "The Limitations of Deep Learning in Adversarial Settings," in *IEEE European Symposium on Security and Privacy (Euro S&P)*. IEEE, 2016, pp. 372–387. 7, 13
- [41] A. Pyrgelis, C. Troncoso, and E. D. Cristofaro, "Knock Knock, Who's There? Membership Inference on Aggregate Location Data," in *Network and Distributed System Security Symposium (NDSS)*. Internet Society, 2018. 4, 12
- [42] S. Rahimian, T. Orekondy, and M. Fritz, "Differential Privacy Defenses and Sampling Attacks for Membership Inference," in *PriML Workshop (PriML)*, 2019. 13
- [43] A. Sablayrolles, M. Douze, C. Schmid, Y. Ollivier, and H. Jégou, "White-box vs Black-box: Bayes Optimal Strategies for Membership Inference," in *International Conference on Machine Learning (ICML)*. JMLR, 2019, pp. 5558–5567. 1, 13
- [44] A. Salem, A. Bhattacharya, M. Backes, M. Fritz, and Y. Zhang, "Updates-Leak: Data Set Inference and Reconstruction Attacks in Online Learning," in *USENIX Security Symposium (USENIX Security)*. USENIX, 2020. 1, 13
- [45] A. Salem, R. Wen, M. Backes, S. Ma, and Y. Zhang, "Dynamic Backdoor Attacks Against Machine Learning Models," CoRR abs/2003.03675, 2020. 13
- [46] A. Salem, Y. Zhang, M. Humbert, P. Berrang, M. Fritz, and M. Backes, "ML-Leaks: Model and Data Independent Membership Inference Attacks and Defenses on Machine Learning Models," in *Network and*

TABLE V: Target model \mathcal{M} with different training set size on each dataset.

Target Model	Target Dataset					
	MNIST	FMNIST	CIFAR10	CIFAR100	GTSRB	Face
\mathcal{M} -0	500	1500	3600	12000	500	400
\mathcal{M} -1	300	1000	2400	9600	400	300
\mathcal{M} -2	200	500	1800	7200	300	250
\mathcal{M} -3	150	300	1200	4800	250	200
\mathcal{M} -4	60	200	800	3600	150	150
\mathcal{M} -5	50	50	400	2400	100	100

Distributed System Security Symposium (NDSS). Internet Society, 2019. 1, 2, 3, 4, 5, 13

- [47] A. Shafahi, W. R. Huang, M. Najibi, O. Suci, C. Studer, T. Dumitras, and T. Goldstein, “Poison Frogs! Targeted Clean-Label Poisoning Attacks on Neural Networks,” in *Annual Conference on Neural Information Processing Systems (NeurIPS)*. NeurIPS, 2018, pp. 6103–6113. 7, 13
- [48] R. Shokri, M. Stronati, C. Song, and V. Shmatikov, “Membership Inference Attacks Against Machine Learning Models,” in *IEEE Symposium on Security and Privacy (S&P)*. IEEE, 2017, pp. 3–18. 1, 2, 3, 4, 5, 10, 12, 13
- [49] C. Song and V. Shmatikov, “Auditing Data Provenance in Text-Generation Models,” in *ACM Conference on Knowledge Discovery and Data Mining (KDD)*. ACM, 2019, pp. 196–206. 13
- [50] R. Tang, M. Du, N. Liu, F. Yang, and X. Hu, “An Embarrassingly Simple Approach for Trojan Attack in Deep Neural Networks,” in *ACM Conference on Knowledge Discovery and Data Mining (KDD)*. ACM, 2020. 13
- [51] F. Tramèr, A. Kurakin, N. Papernot, I. Goodfellow, D. Boneh, and P. McDaniel, “Ensemble Adversarial Training: Attacks and Defenses,” in *International Conference on Learning Representations (ICLR)*, 2017. 7, 13
- [52] F. Tramèr, F. Zhang, A. Juels, M. K. Reiter, and T. Ristenpart, “Stealing Machine Learning Models via Prediction APIs,” in *USENIX Security Symposium (USENIX Security)*. USENIX, 2016, pp. 601–618. 13
- [53] B. Wang and N. Z. Gong, “Stealing Hyperparameters in Machine Learning,” in *IEEE Symposium on Security and Privacy (S&P)*. IEEE, 2018, pp. 36–52. 13
- [54] B. Wang, Y. Yao, S. Shan, H. Li, B. Viswanath, H. Zheng, and B. Y. Zhao, “Neural Cleanse: Identifying and Mitigating Backdoor Attacks in Neural Networks,” in *IEEE Symposium on Security and Privacy (S&P)*. IEEE, 2019, pp. 707–723. 13
- [55] T.-W. Weng, H. Zhang, H. Chen, Z. Song, C.-J. Hsieh, L. Daniel, D. S. Boning, and I. S. Dhillon, “Towards Fast Computation of Certified Robustness for ReLU Networks,” in *International Conference on Machine Learning (ICML)*. JMLR, 2018, pp. 5273–5282. 9
- [56] Z. Yang, B. Shao, B. Xuan, E.-C. Chang, and F. Zhang, “Defending Model Inversion and Membership Inference Attacks via Prediction Purification,” CoRR abs/2005.03915, 2020. 13
- [57] S. Yeom, I. Giacomelli, M. Fredrikson, and S. Jha, “Privacy Risk in Machine Learning: Analyzing the Connection to Overfitting,” in *IEEE Computer Security Foundations Symposium (CSF)*. IEEE, 2018, pp. 268–282. 1, 2, 13
- [58] R. Zhai, C. Dan, D. He, H. Zhang, B. Gong, P. Ravikumar, C.-J. Hsieh, and L. Wang, “MACER: Attack-free and Scalable Robust Training via Maximizing Certified Radius,” in *International Conference on Learning Representations (ICLR)*, 2020. 9

VIII. APPENDIX

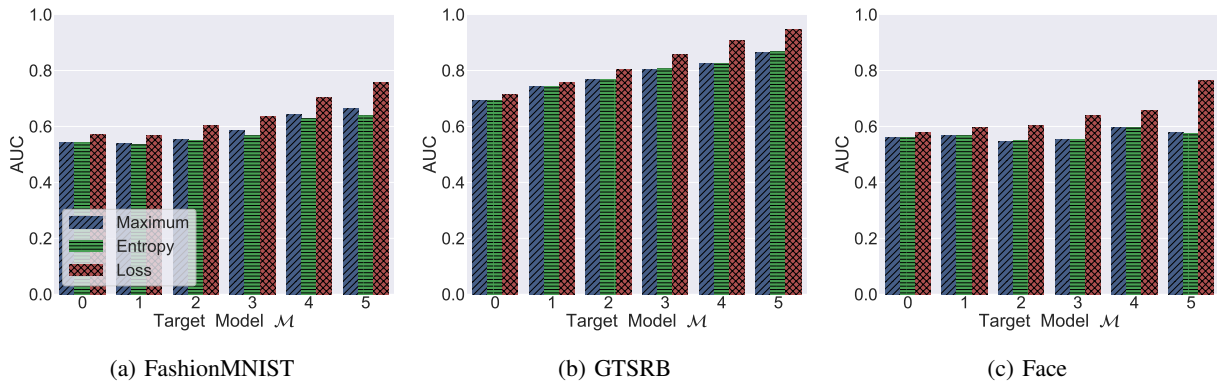


Fig. 14: Attack AUC for three different statistical measures. The x-axis represents the target model being attacked and the y-axis represents the AUC score.

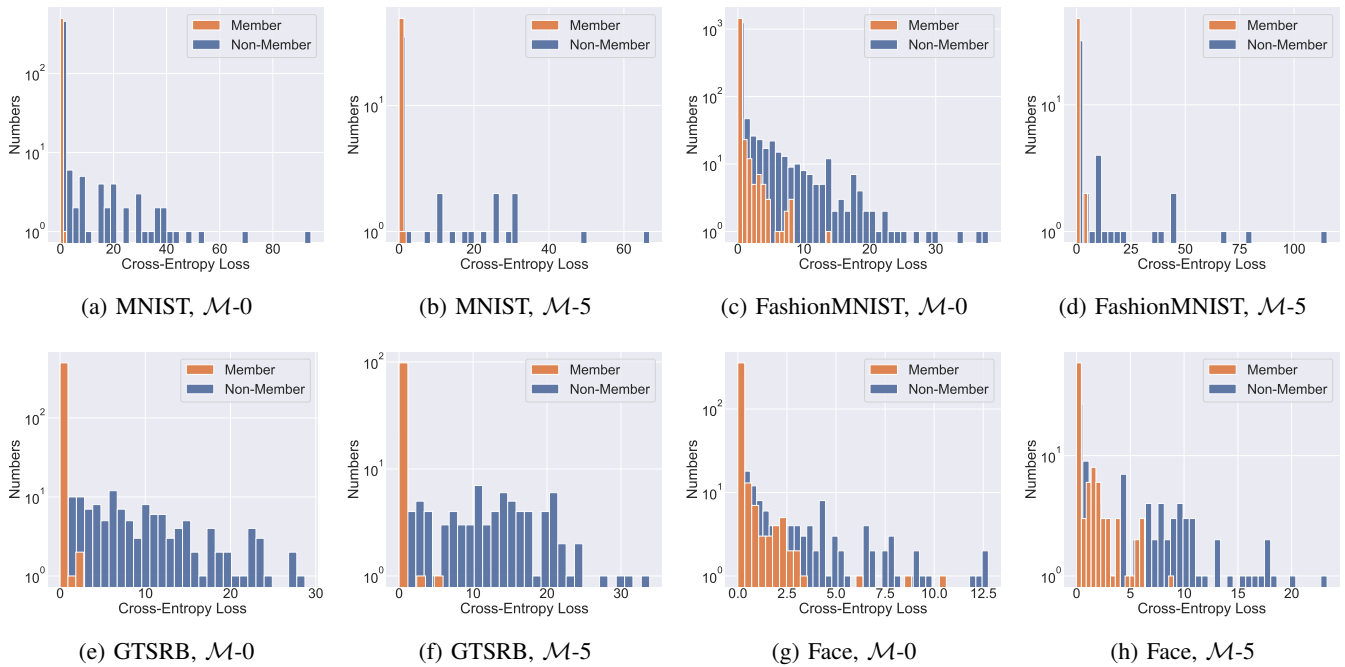


Fig. 15: The cross entropy loss distribution obtained from the shadow model. The x-axis represent the loss value and the y-axis represent the number of the loss.

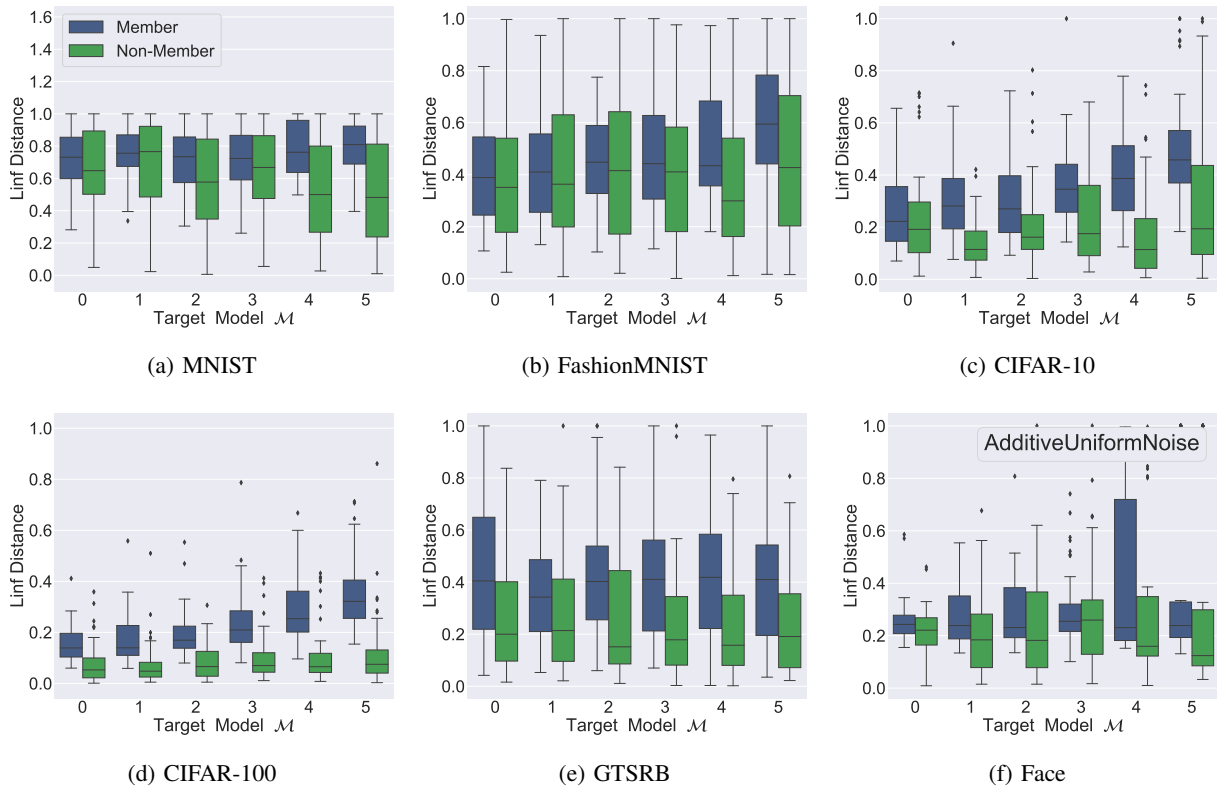


Fig. 16: L_∞ distance between the original samples and the corresponding perturbed samples generated by the AdditiveUniform-Noise attack. The x-axis represents the target model being attacked and the y-axis represent the L_∞ distance

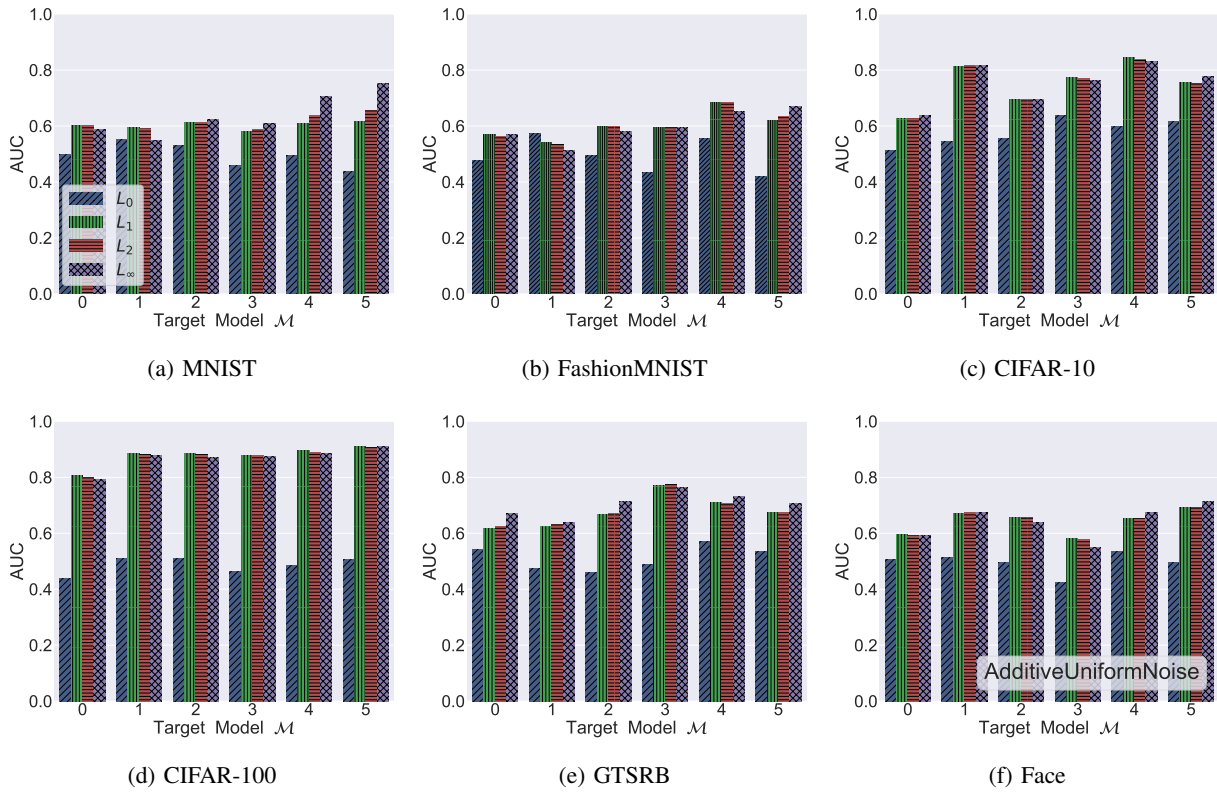


Fig. 17: Attack AUC for four different L_p distances to measure the distance between the original samples and the corresponding perturbed samples generated by the AdditiveUniformNoise attack. The x-axis represents the target model being attacked and the y-axis represent the AUC score.